

Title	Interaction of two counterpropagating laser beams with vacuum
Author(s)	Monden, Y.; Kodama, R.
Citation	Physical Review A - Atomic, Molecular, and Optical Physics. 2012, 86(3), p. 033810
Version Type	VoR
URL	<a href="https://hdl.handle.net/11094/98318">https://hdl.handle.net/11094/98318</a>
rights	Copyright 2012 by the American Physical Society
Note	

*Osaka University Knowledge Archive : OUKA*

<https://ir.library.osaka-u.ac.jp/>

Osaka University

## Interaction of two counterpropagating laser beams with vacuum

Y. Monden<sup>1,\*</sup> and R. Kodama<sup>1,2</sup>

<sup>1</sup>Graduate School of Engineering, Osaka University, 2-1 Yamada-oka, Suita, Osaka 565-0871, Japan

<sup>2</sup>Photon Pioneers Center, Osaka University, 2-1 Yamada-Oka, Suita, Osaka 565-0871, Japan

(Received 23 March 2012; published 7 September 2012)

We have investigated the interaction of two counterpropagating focused laser beams with vacuum at electro-magnetic-field strengths far below the Schwinger limit. Unlike the case of a single beam, the polarization and magnetization in vacuum that interacts with the two laser beams are mainly generated by electro-magnetic-field components parallel to the electromagnetic field of the incident laser light. This results in much greater polarization and magnetization being generated than for a single beam. The number of photons radiated from a vacuum when counterpropagating beams were used was more than 3 orders of magnitude higher than when a single beam was used for the same laser power.

DOI: [10.1103/PhysRevA.86.033810](https://doi.org/10.1103/PhysRevA.86.033810)

PACS number(s): 42.50.Xa, 42.65.-k

Interactions between ultraintense laser light and vacuum are expected to open up new areas in the field of high-field physics [1]. Such interactions typically generate electron-positron pairs from vacuum when the laser light intensity is close to the Schwinger limit  $I_{\text{sch}} = cE_{\text{sch}}^2/4\pi \sim 10^{29}$  W/cm<sup>2</sup>, where  $c$  is the speed of light,  $E_{\text{sch}} = m^2c^3/e\hbar$  is the field strength of the Schwinger limit,  $e$  is the elementary charge,  $m$  is the electron mass, and  $\hbar$  is the reduced Planck constant [2]. This phenomenon is caused by the energy corresponding to the masses of the produced particles being transferred to the vacuum. However, a vacuum irradiated by optical laser light is expected to exhibit nonlinear optical properties even at intensities far below the Schwinger limit since the interaction of the light with virtual electron-positron pairs in the vacuum induces nonlinear polarization and magnetization in the vacuum. Recent calculations, based on a model of the electromagnetic field of focused laser light [3] in which the effect of an angular aperture ( $\theta$  in Fig. 1) is accurately considered, predict that the nonlinear polarization and magnetization in a vacuum irradiated by a focused laser beam increase nonlinearly with increasing angular aperture, resulting in a nonlinear increase in the energy of light radiated from the vacuum [4].

Another method for increasing the polarization and magnetization is to superpose two counterpropagating beams. In generating the polarization and magnetization, the Lorentz invariants  $\mathcal{F} = (|\mathbf{B}|^2 - |\mathbf{E}|^2)/2$  and  $\mathcal{G} = \mathbf{E} \cdot \mathbf{B}$  of the electric field  $\mathbf{E}$  and magnetic field  $\mathbf{B}$  of the laser light are critical quantities [4]. Although the magnitudes of  $\mathcal{F}$  and  $\mathcal{G}$  increase with increasing angular aperture, they are much smaller than  $|\mathbf{E}|^2$  and  $|\mathbf{B}|^2$ , even for extremely large angular apertures of over 100° in the case of a single laser beam. On the other hand, for counterpropagating beams focused at the same point, the Lorentz invariants become much larger than those of a single beam:  $\mathcal{F}$  becomes up to about  $|\mathbf{E}|^2$  for beams with the same polarization [Fig. 1(a)], and  $\mathcal{G}$  becomes up to about  $|\mathbf{E}||\mathbf{B}|$  when the beams have perpendicular polarizations [Fig. 1(b)]. For this reason, the interactions of vacuum with counterpropagating beams have been studied theoretically [5–8], and schemes to probe the vacuum irradiated by counterpropagating

beams with an x-ray beam have been proposed [9,10]. To put the schemes into experiments, it is necessary to use an x-ray free-electron laser and high-power laser at the same time. However, it would be possible to study the interaction of vacuum with counterpropagating beams focused by a large angular aperture without the probe beam, and many more photons are expected to be radiated from a vacuum than for a single beam.

Here, we theoretically investigate the interaction of two counterpropagating focused laser beams with a vacuum using a similar method to that in Ref. [4]. The polarization and magnetization in a vacuum that interacts with laser light increase when two beams are superposed due to an increase in the Lorentz invariants. Calculations of the wave equations in vacuum that contain correction terms for quantum electrodynamics (QED) predict that using counterpropagating beams increase the number of radiated photons by more than 3 orders of magnitude relative to that for a single beam.

The effective Lagrangian density  $\mathcal{L}$  of an electromagnetic field in vacuum [2,11], which is valid for fields with wavelengths much longer than the electron Compton wavelength and field strengths below  $E_{\text{sch}}$  [12], is represented by the sum of the conventional Lagrangian density of classical electrodynamics  $\mathcal{L}_{\text{cl}}$  and the QED correction term  $\mathcal{L}'$ :  $\mathcal{L} = \mathcal{L}_{\text{cl}} + \mathcal{L}'$ .  $\mathcal{L}'$  is described in terms of  $\mathcal{F}$  and  $\mathcal{G}$  by the following expansion [12]:

$$\begin{aligned} \mathcal{L}' &= \mathcal{L}_1 + \mathcal{L}_2 + \dots \\ &= \frac{\alpha(4\mathcal{F}^2 + 7\mathcal{G}^2)}{360\pi^2 E_{\text{sch}}^2} - \frac{\alpha\mathcal{F}(8\mathcal{F}^2 + 13\mathcal{G}^2)}{630\pi^2 E_{\text{sch}}^4} + \dots, \end{aligned} \quad (1)$$

where  $\alpha = e^2/\hbar c$  is the fine-structure constant. The polarization  $\mathbf{P}$  and the magnetization  $\mathbf{M}$  in vacuum are obtained from  $\mathcal{L}'$  in the forms of  $\mathbf{P} = \mathbf{P}_1 + \mathbf{P}_2 + \dots$  and  $\mathbf{M} = \mathbf{M}_1 + \mathbf{M}_2 + \dots$ , where  $\mathbf{P}_m$  and  $\mathbf{M}_m$  are given by the  $m$ th term of  $\mathcal{L}'$ , respectively. The lowest-order terms  $\mathbf{P}_1$  and  $\mathbf{M}_1$  are given by

$$\mathbf{P}_1 = \xi(7\mathcal{G}\mathbf{B} - 4\mathcal{F}\mathbf{E}), \quad \mathbf{M}_1 = \xi(7\mathcal{G}\mathbf{E} + 4\mathcal{F}\mathbf{B}), \quad (2)$$

where  $\xi = \alpha/180\pi^2 E_{\text{sch}}^2$ .

To accurately consider the vector character of the electromagnetic field of focused laser light for a large angular aperture, we use the representation based on the vector diffraction theory of Richards and Wolf [3]. In this representation, the

\*ymonden@ef.eie.eng.osaka-u.ac.jp

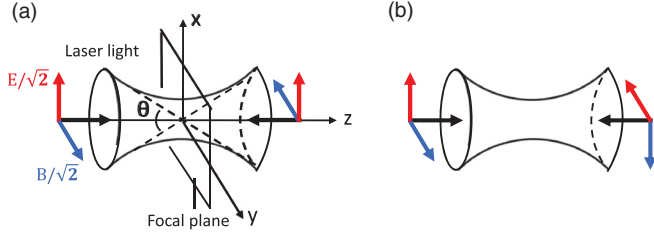


FIG. 1. (Color) Geometric configurations of two counterpropagating beams obtained by splitting one beam with electric- and magnetic-field amplitudes of  $E$  and  $B$  into two beams with electric- and magnetic-field amplitudes of  $E/\sqrt{2}$  and  $B/\sqrt{2}$  for (a) the same polarization and (b) mutually perpendicular polarizations.

electric field  $\mathbf{E}_L(\mathbf{r}, t)$  and the magnetic field  $\mathbf{B}_L(\mathbf{r}, t)$ , at a point  $\mathbf{r} = (x, y, z)$  near the focus and at time  $t$  of a single laser beam with a frequency  $\omega$ , are expressed by  $\mathbf{E}_L(\mathbf{r}, t) = \text{Re}\{\mathbf{e}(\mathbf{r})e^{-i\omega t}\}$  and  $\mathbf{B}_L(\mathbf{r}, t) = \text{Re}\{\mathbf{b}(\mathbf{r})e^{-i\omega t}\}$ , where  $\mathbf{e}(\mathbf{r})$  and  $\mathbf{b}(\mathbf{r})$  are the time-independent parts of  $\mathbf{E}_L(\mathbf{r}, t)$  and  $\mathbf{B}_L(\mathbf{r}, t)$ , respectively, and  $\text{Re}$  denotes the real part. Defining  $x$  and  $y$  axes with an origin at the focus as the directions of the electric and magnetic fields of the incident light, respectively, and the  $z$  axis as the propagation direction of the light, the Cartesian components of  $\mathbf{e}(\mathbf{r})$  and  $\mathbf{b}(\mathbf{r})$  are given by [3]

$$\begin{bmatrix} e_x(\rho, \varphi, z) \\ e_y(\rho, \varphi, z) \\ e_z(\rho, \varphi, z) \end{bmatrix} = A \begin{bmatrix} -i\{I_0(\rho, z) + I_2(\rho, z) \cos 2\varphi\} \\ -iI_2(\rho, z) \sin 2\varphi \\ -2I_1(\rho, z) \cos \varphi \end{bmatrix}, \quad (3)$$

$$\begin{bmatrix} b_x(\rho, \varphi, z) \\ b_y(\rho, \varphi, z) \\ b_z(\rho, \varphi, z) \end{bmatrix} = A \begin{bmatrix} -iI_2(\rho, z) \sin 2\varphi \\ -i\{I_0(\rho, z) - I_2(\rho, z) \cos 2\varphi\} \\ -2I_1(\rho, z) \sin \varphi \end{bmatrix},$$

where  $A = \pi f E_0 / \lambda$ ,  $f$  is the focal length of the focusing optics,  $E_0$  is the electric-field amplitude of the incident light, and  $\lambda$  is the wavelength. Here,  $(\rho, \varphi, z)$  are cylindrical

coordinates, and

$$\begin{aligned} I_0(\rho, z) &= \int_0^{\theta/2} d\theta' I_0(\theta') \cos^{1/2} \theta' \sin \theta' (1 + \cos \theta') \\ &\quad \times J_0(k\rho \sin \theta') e^{ikz \cos \theta'}, \\ I_1(\rho, z) &= \int_0^{\theta/2} d\theta' I_0(\theta') \cos^{1/2} \theta' \sin^2 \theta' J_1(k\rho \sin \theta') \\ &\quad \times e^{ikz \cos \theta'}, \\ I_2(\rho, z) &= \int_0^{\theta/2} d\theta' I_0(\theta') \cos^{1/2} \theta' \sin \theta' (1 - \cos \theta') \\ &\quad \times J_2(k\rho \sin \theta') e^{ikz \cos \theta'}, \end{aligned} \quad (4)$$

where  $I_0(\theta')$  is a function related to the amplitude distribution of the electric field of the incident light [13,14] and  $J_n(k\rho \sin \theta')$  ( $n = 0, 1, 2$ ) is the Bessel function of the first kind of order  $n$ . The time-independent parts of  $\mathbf{E}_{L\parallel}(\mathbf{r}, t) = \text{Re}\{\mathbf{e}_{\parallel}(\mathbf{r})e^{-i\omega t}\}$  and  $\mathbf{E}_{L\perp}(\mathbf{r}, t) = \text{Re}\{\mathbf{e}_{\perp}(\mathbf{r})e^{-i\omega t}\}$ , which are the electric fields of the counterpropagating focused beams with the same polarizations and of the beams polarized perpendicularly to each other, respectively, are given by

$$\begin{bmatrix} e_{\parallel,x}(\rho, \varphi, z) \\ e_{\parallel,y}(\rho, \varphi, z) \\ e_{\parallel,z}(\rho, \varphi, z) \end{bmatrix} = \begin{bmatrix} e_x(\rho, \varphi, z) + e_x(\rho, -\varphi, -z) \\ e_y(\rho, \varphi, z) - e_y(\rho, -\varphi, -z) \\ e_z(\rho, \varphi, z) - e_z(\rho, -\varphi, -z) \end{bmatrix}, \quad (5)$$

$$\begin{bmatrix} e_{\perp,x}(\rho, \varphi, z) \\ e_{\perp,y}(\rho, \varphi, z) \\ e_{\perp,z}(\rho, \varphi, z) \end{bmatrix} = \begin{bmatrix} e_x(\rho, \varphi, z) - e_y(\rho, \pi/2 - \varphi, -z) \\ e_y(\rho, \varphi, z) - e_x(\rho, \pi/2 - \varphi, -z) \\ e_z(\rho, \varphi, z) - e_z(\rho, \pi/2 - \varphi, -z) \end{bmatrix}.$$

The magnetic fields of the beams are similarly given. Using these expressions for the electromagnetic fields,  $(\mathcal{F}_L(\mathbf{r}, t), \mathcal{G}_L(\mathbf{r}, t))$ ,  $(\mathcal{F}_{L\parallel}(\mathbf{r}, t), \mathcal{G}_{L\parallel}(\mathbf{r}, t))$ , and  $(\mathcal{F}_{L\perp}(\mathbf{r}, t), \mathcal{G}_{L\perp}(\mathbf{r}, t))$ , which are the Lorentz invariants of  $(\mathbf{E}_L(\mathbf{r}, t), \mathbf{B}_L(\mathbf{r}, t))$ ,  $(\mathbf{E}_{L\parallel}(\mathbf{r}, t), \mathbf{B}_{L\parallel}(\mathbf{r}, t))$ , and  $(\mathbf{E}_{L\perp}(\mathbf{r}, t), \mathbf{B}_{L\perp}(\mathbf{r}, t))$ , respectively, are obtained as follows:

$$\begin{aligned} \mathcal{F}_L(\rho, \varphi, z, t) &= \mathcal{G}_L(\rho, \varphi - \pi/4, z, t) = -A^2 \cos 2\varphi [ |I_1|^2 + \text{Re}\{I_0 I_2^* + (I_1^2 - I_0 I_2) e^{-i2\omega t}\} ], \\ \mathcal{F}_{L\parallel}(\rho, \varphi, z, t) &= -A^2 [ \text{Re}\{I_0^2 - 2I_1^2 + I_2^2\} + 2(|I_1|^2 + \text{Re}\{I_0 I_2^*\}) \cos 2\varphi - (|I_0|^2 + 2|I_1|^2 + |I_2|^2 \\ &\quad - 2 \text{Re}\{I_1^2 - I_0 I_2\} \cos 2\varphi) \cos 2\omega t ], \\ \mathcal{G}_{L\perp}(\rho, \varphi, z, t) &= -A^2 [ \text{Re}\{I_0^2 + 2I_1^2 + I_2^2\} - 2(|I_1|^2 + \text{Re}\{I_0 I_2^*\}) \sin 2\varphi \\ &\quad - (|I_0|^2 - 2|I_1|^2 + |I_2|^2 + 2 \text{Re}\{I_1^2 - I_0 I_2\} \sin 2\varphi) \cos 2\omega t ], \\ \mathcal{F}_{L\perp}(\rho, \varphi, z, t) &= \mathcal{G}_{L\parallel}(\rho, \varphi - \pi/4, z, t) = -2A^2 \text{Im}\{I_1^2 - I_0 I_2\} \cos 2\varphi \sin 2\omega t, \end{aligned} \quad (6)$$

where the asterisk indicates the complex conjugate,  $\text{Im}$  denotes the imaginary part, and the variables of  $I_n(\rho, z)$  are omitted. From Eq. (6), it is found that the terms related to  $I_0^2(\rho, z)$  or  $|I_0(\rho, z)|^2$  are not contained in  $\mathcal{F}_L(\mathbf{r}, t)$  and  $\mathcal{G}_L(\mathbf{r}, t)$  but are contained in  $\mathcal{F}_{L\parallel}(\mathbf{r}, t)$  and  $\mathcal{G}_{L\perp}(\mathbf{r}, t)$ . This indicates that, although the Lorentz invariants of a single beam mainly originate from the longitudinal  $z$  components of the electromagnetic field [4],  $\mathcal{F}_{L\parallel}(\mathbf{r}, t)$  and  $\mathcal{G}_{L\perp}(\mathbf{r}, t)$  are mainly

due to the components parallel to the electromagnetic field of the incident light, which contain  $I_0(\rho, z)$  [see Eq. (3)] and are much larger than the longitudinal components, even near the focus. The Lorentz invariants of the counterpropagating beams are then expected to be much larger than those of the single beam.

Considering the above-mentioned electromagnetic fields, the amplitudes of  $\mathbf{P}_2$  and  $\mathbf{M}_2$  will be over 3 orders of

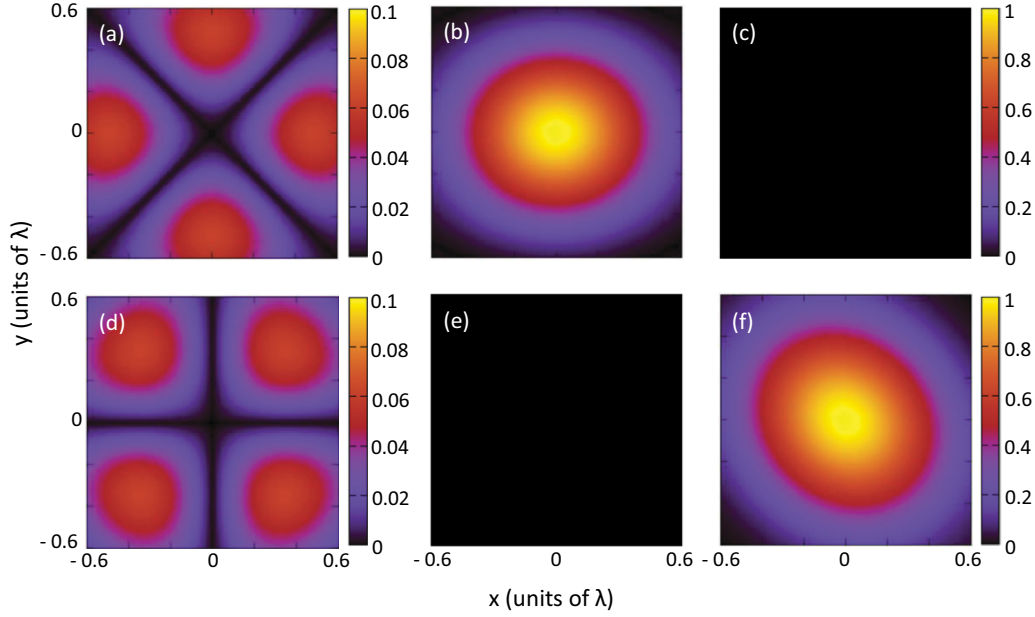


FIG. 2. (Color) Distributions of the Lorentz invariants (a)  $|\langle \mathcal{F}_L(\mathbf{r}, t) \rangle|$ , (b)  $|\langle \mathcal{F}_{L||}(\mathbf{r}, t) \rangle|$ , (c)  $|\langle \mathcal{F}_{L\perp}(\mathbf{r}, t) \rangle|$ , (d)  $|\langle \mathcal{G}_L(\mathbf{r}, t) \rangle|$ , (e)  $|\langle \mathcal{G}_{L||}(\mathbf{r}, t) \rangle|$ , and (f)  $|\langle \mathcal{G}_{L\perp}(\mathbf{r}, t) \rangle|$  in the focal plane for  $\theta = 100^\circ$ . The  $x$  and  $y$  axes are expressed in units of  $\lambda$ . The Lorentz invariants are normalized to the maximum value of  $|\langle \mathcal{F}_{L||}(\mathbf{r}, t) \rangle|$ , which is equal to that of  $|\langle \mathcal{G}_{L\perp}(\mathbf{r}, t) \rangle|$ .

magnitude smaller than those of  $\mathbf{P}_1$  and  $\mathbf{M}_1$  for peak laser intensities below  $10^{26}$  W/cm<sup>2</sup>. The contributions of  $\mathbf{P}_2$ ,  $\mathbf{M}_2$ , and higher components are then negligible since we are considering light with peak intensities much lower than  $I_{\text{sch}}$ . In the calculations, we consider only the components with a fundamental frequency  $\omega$  of the lowest-order terms  $\mathbf{P}_1$  and  $\mathbf{M}_1$  in Eq. (2).

We assume that the intensity distribution of the incident light is Gaussian, and  $\lambda = 1 \mu\text{m}$ . Figures 2(a)–2(f), respectively, show the distributions of  $|\langle \mathcal{F}_L(\mathbf{r}, t) \rangle|$ ,  $|\langle \mathcal{F}_{L||}(\mathbf{r}, t) \rangle|$ ,  $|\langle \mathcal{F}_{L\perp}(\mathbf{r}, t) \rangle|$ ,  $|\langle \mathcal{G}_L(\mathbf{r}, t) \rangle|$ ,  $|\langle \mathcal{G}_{L||}(\mathbf{r}, t) \rangle|$ , and  $|\langle \mathcal{G}_{L\perp}(\mathbf{r}, t) \rangle|$  in the focal plane for the angular aperture  $\theta = 100^\circ$ , where the angle brackets denote the time-averaged value. Figure 2 shows that the maximum values of  $|\langle \mathcal{F}_{L||}(\mathbf{r}, t) \rangle|$  and  $|\langle \mathcal{G}_{L\perp}(\mathbf{r}, t) \rangle|$  are more than 1 order of magnitude larger than those of  $|\langle \mathcal{F}_L(\mathbf{r}, t) \rangle|$  and  $|\langle \mathcal{G}_L(\mathbf{r}, t) \rangle|$ . Figures 3(a)–3(c), respectively, show the distributions of  $\sqrt{\langle |\mathbf{P}_L(\mathbf{r}, t)|^2 \rangle}$ ,  $\sqrt{\langle |\mathbf{P}_{L||}(\mathbf{r}, t)|^2 \rangle}$ , and  $\sqrt{\langle |\mathbf{P}_{L\perp}(\mathbf{r}, t)|^2 \rangle}$ , which correspond to the amplitudes of the polarizations,

in the focal plane for  $\theta = 100^\circ$ . Here,  $\mathbf{P}_L(\mathbf{r}, t)$ ,  $\mathbf{P}_{L||}(\mathbf{r}, t)$ , and  $\mathbf{P}_{L\perp}(\mathbf{r}, t)$  are the polarizations generated by the electromagnetic fields  $(\mathbf{E}_L(\mathbf{r}, t), \mathbf{B}_L(\mathbf{r}, t))$ ,  $(\mathbf{E}_{L||}(\mathbf{r}, t), \mathbf{B}_{L||}(\mathbf{r}, t))$ , and  $(\mathbf{E}_{L\perp}(\mathbf{r}, t), \mathbf{B}_{L\perp}(\mathbf{r}, t))$ , respectively. Although  $|\langle \mathcal{G}_{L||}(\mathbf{r}, t) \rangle|$  and  $|\langle \mathcal{F}_{L\perp}(\mathbf{r}, t) \rangle|$  vanish, the amplitudes of  $\mathbf{P}_{L||}(\mathbf{r}, t)$  and  $\mathbf{P}_{L\perp}(\mathbf{r}, t)$  become much larger than that of  $\mathbf{P}_L(\mathbf{r}, t)$ . Moreover, the maximum amplitude of  $\mathbf{P}_{L\perp}(\mathbf{r}, t)$  is larger than that of  $\mathbf{P}_{L||}(\mathbf{r}, t)$  due to the difference between the coefficients of the first and second terms in Eq. (2). Similar results are obtained for the magnetization.

The electric field  $\mathbf{E}_r(\mathbf{r}, t)$  and magnetic field  $\mathbf{B}_r(\mathbf{r}, t)$  of light radiated from the vacuum irradiated by laser light are obtained by solving the wave equations given by the Lagrangian density including the QED correction term  $\mathcal{L}'$  [4]. In calculations, the contributions of  $\mathbf{E}_r(\mathbf{r}, t)$  and  $\mathbf{B}_r(\mathbf{r}, t)$  to the polarization and magnetization can be neglected because the radiated light has a much lower field strength than the focused laser light. The number of photons of the radiated light per laser shot is equal to

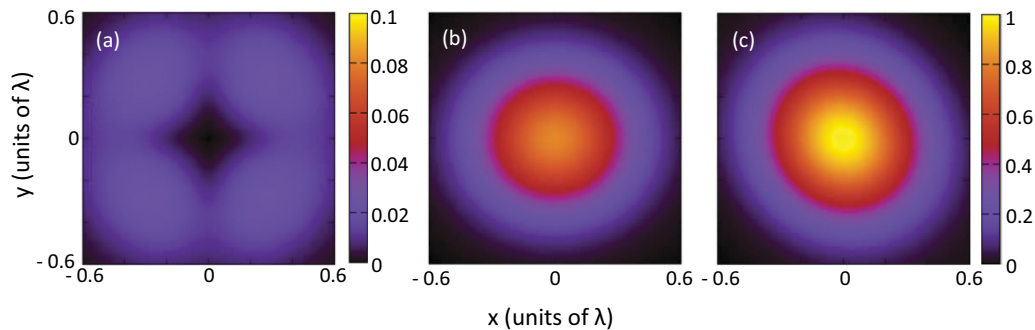


FIG. 3. (Color) Distributions of the amplitudes of the polarizations (a)  $\mathbf{P}_L(\mathbf{r}, t)$ , (b)  $\mathbf{P}_{L||}(\mathbf{r}, t)$ , and (c)  $\mathbf{P}_{L\perp}(\mathbf{r}, t)$  in the focal plane for  $\theta = 100^\circ$  where the amplitude of  $\mathbf{P}(\mathbf{r}, t)$  is given by  $\sqrt{\langle |\mathbf{P}(\mathbf{r}, t)|^2 \rangle}$ . The  $x$  and  $y$  axes are expressed in units of  $\lambda$ . The amplitudes are normalized to the maximum value of  $\sqrt{\langle |\mathbf{P}_{L\perp}(\mathbf{r}, t)|^2 \rangle}$ .

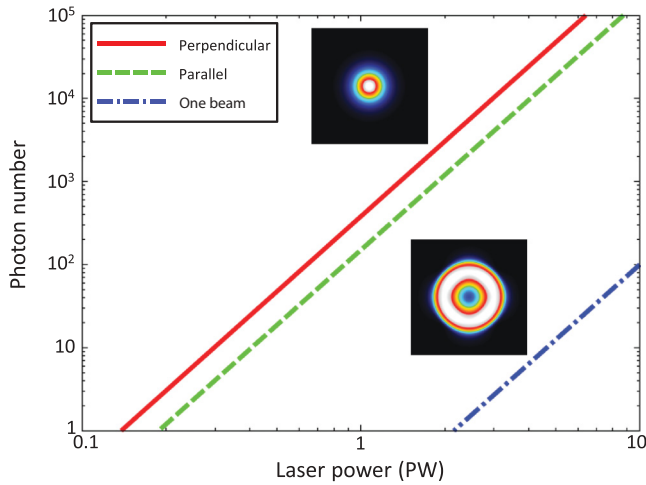


FIG. 4. (Color) The number of photons of the radiated light as a function of laser power for  $\tau = 100$  fs and the intensity distributions of the radiated light in the  $x$ - $y$  plane located  $500\lambda = 500 \mu\text{m}$  from the focal plane in the direction of the  $z$  axis for upper figure: two counterpropagating beams and lower figure: a single beam. The intensity distributions are normalized to their peak values, and the  $f$  number is assumed to be 0.4 (i.e.,  $\theta \simeq 103^\circ$ ). In the case of two beams, the laser power indicates the total power of the beams.

the total energy of the radiated light over a laser-pulse duration  $\tau$  divided by the energy of a single photon; the laser pulse is assumed to be rectangular as in Ref. [4].

Figure 4 shows the total number of photons of the radiated light with the fundamental frequency  $\omega$  as a function of the laser power for  $\tau = 100$  fs and an  $f$  number of  $f/\# = 0.4$  ( $\theta \simeq 103^\circ$ ), which has already been realized by using focusing plasma optics [15], and the intensity distributions of the radiated light in the  $x$ - $y$  plane located  $500\lambda = 500 \mu\text{m}$  from the focal plane in the direction of the  $z$  axis for two counterpropagating beams and a single beam. For the counterpropagating beams, the laser power indicates the total power of the beams. The solid, dashed, and dot-dashed lines in Fig. 4 indicate the calculation results for counterpropagating beams with the same polarizations, counterpropagating beams polarized perpendicularly to each other, and a single

beam, respectively. The counterpropagating beams and the single beam give quite different distributions because the distributions reflect those of the polarization shown in Fig. 3. Comparison of the results for the counterpropagating beams with the two different polarizations with the same laser power reveals that the number of the radiated photons increases by a factor of approximately 2 when the polarization direction of one beam is rotated by  $90^\circ$ . More importantly, by using the counterpropagating beams, the number of radiated photons is more than 3 orders of magnitude greater than that for a single beam with the same laser power, exceeding 100 at 1 PW.

In both cases of two counterpropagating beams and a single beam, there are a few percent of the radiated photons polarized perpendicularly to the incident laser light, which could be distinguished from the incident photons of the laser light. In the case of the counterpropagating beams with a fixed laser power, the number of the photons polarized perpendicularly to the incident light increases with  $\theta$ , although the total photon number is nearly independent of  $\theta$ . For example, the number of photons polarized perpendicularly to the incident light for  $\theta = 103^\circ$  is more than 2 orders of magnitude larger than that for  $\theta = 14^\circ$  ( $f/\# \simeq 4$ ).

In this paper, we investigated the interaction of counterpropagating laser beams with a vacuum. The Lorentz invariants of the electromagnetic field of the counterpropagating beams are more than 1 order of magnitude larger than those of a single beam, which leads to a large increase in the polarization and magnetization in a vacuum. Consequently, the number of photons radiated from the vacuum irradiated by the two counterpropagating beams increases by more than 3 orders of magnitude compared to that for a single beam at the same laser power, and it exceeds 100 at 1 PW. This result indicates that using counterpropagating laser light focused by large angular aperture is an efficient way to detect nonlinear optical properties in vacuum with practical intensities.

This work was supported by the Global COE Program, “Center for Electronic Devices Innovation,” the JST-CREST Program, “High Energy Density Plasma Photonics,” and the Photon Frontier Network Program, “Photon Pioneers Center in Osaka University.”

[1] Extreme Light Infrastructure (ELI), *ELI Scientific Case* [http://www.extreme-light-infrastructure.eu/ELI-scientific-case\\_2\\_4.php](http://www.extreme-light-infrastructure.eu/ELI-scientific-case_2_4.php).  
 [2] J. Schwinger, *Phys. Rev.* **82**, 664 (1951).  
 [3] B. Richards and E. Wolf, *Proc. R. Soc. London, Ser. A* **253**, 358 (1959).  
 [4] Y. Monden and R. Kodama, *Phys. Rev. Lett.* **107**, 073602 (2011).  
 [5] N. B. Narozhny, S. S. Bulanov, V. D. Mur, and V. S. Popov, *JETP Lett.* **80**, 382 (2004).  
 [6] S. S. Bulanov, N. B. Narozhny, V. D. Mur, and V. S. Popov, *JETP* **102**, 9 (2006).  
 [7] D. B. Blaschke, A. V. Prozorkevich, C. D. Roberts, S. M. Schmidt, and S. A. Smolyansky, *Phys. Rev. Lett.* **96**, 140402 (2006).

[8] M. Marklund and J. Lundin, *Eur. Phys. J. D* **55**, 319 (2009).  
 [9] A. Di Piazza, K. Z. Hatsagortsyan, and C. H. Keitel, *Phys. Rev. Lett.* **97**, 083603 (2006).  
 [10] T. Heinzl *et al.*, *Opt. Commun.* **267**, 318 (2006).  
 [11] W. Heisenberg and H. Euler, *Z. Phys.* **98**, 714 (1936).  
 [12] V. B. Berestetskii, E. M. Lifshitz, and L. P. Pitaevskii, *Quantum Electrodynamics* (Pergamon, Oxford, 1982).  
 [13] J. J. Stamnes, *Waves in Focal Regions* (Hilger, Bristol, 1986).  
 [14] K. S. Youngworth and T. G. Brown, *Opt. Express* **7**, 77 (2000).  
 [15] M. Nakatsutsumi *et al.*, *Opt. Lett.* **35**, 2314 (2010).